

## Hydrogen Permeation Through X56 Pipeline Steel in Atmospheric Environment and Its Implication on SCC

Guo Yi, Chuanbo Zheng\*

School of material science & engineering of Jiangsu University of Science & Technology, Jiangsu, 212003;

\*E-mail: [Chuanbo.zheng@gmail.com](mailto:Chuanbo.zheng@gmail.com)

*Received:* 29 August 2012 / *Accepted:* 2 October 2012 / *Published:* 1 November 2012

---

Stress corrosion cracking and Hydrogen permeation behavior of X56 grade pipeline steel in simulated atmospheric environment containing SO<sub>2</sub> was investigated. The results show that, 1) Hydrogen permeation current can be divided into 3 parts in atmospheric environment containing SO<sub>2</sub>. The mainly hydrogen resource is different according to the reaction mechanism. 2) The surface hydrogen ions concentration decrease with time. And this indicates that the surface hydrogen concentration decrease with the formation of corrosion rust. 3) Slow strain rate test (SSRT) shows that SCC sensitivity of X56 increase with the concentration of SO<sub>2</sub> due to the passivation film dissolves and hydrogen permeation rate increasing.

---

**Keywords:** Hydrogen permeation current, corrosion weight loss, surface hydrogen concentration, autocatalysis of SO<sub>4</sub><sup>2-</sup>, SCC

### 1. INTRODUCTION

Atmospheric corrosion and environmental degradation processes are ubiquitous and result in significant costs throughout the world. And the hydrogen induced cracking and hydrogen embrittlement have long been recognized as a serious problem for the petroleum and petrochemical industries, particularly in high strength and stainless steel [1-5]. The delayed fracture or hydrogen embrittlement (HE) of high strength steels has been reported to take place in atmospheric environment. Most of researchers do not pay attention to or neglect the hydrogen permeation into steels under the atmospheric conditions, since the steels are much less susceptible to HE than the high strength steels under the atmospheric conditions, and the reduction reaction of proton is considered to be neglected compared to the other cathodic reduction reactions such as the dissolved oxygen reduction reaction. It is recently that the hydrogen permeation during atmospheric corrosion was studied concerning the

environment sensitive fracture for such steels [6-8]. And X56 steel is a pipeline steel which is used in petroleum and petrochemical industries. In the petroleum and petrochemical industries, the existence of  $\text{SO}_2$  and  $\text{H}_2\text{S}$  is a big problem for exploitation and transport.

Usually, the atmospheric environment was simulated by dropping corrosion solution onto the specimen surface. In this paper, the atmospheric environment was simulated by self-evaporation of corrosion solution, which is more close to the real one. And in this paper, the electrochemical permeation technique was used to study the behavior of hydrogen permeation into X56 grade pipeline steels and stress corrosion cracking under a simulated atmospheric environment containing  $\text{SO}_2$ . And the corrosion behavior also was studied by the weight loss measurement.

## 2. EXPERIMENTAL METHOD

### 2.1. Materials and specimen

The material for the study was a commercial X56 steel with a chemical composition (wt%) as follows, C: 0.15, Mn: 1.46, Si: 0.38, O: 0.0020, P: 0.011, S: 0.005, N: 0.0022. Circular plate specimen of 40mm in diameter and 0.5mm in thickness was used as the work electrode. The specimens were polished with emery paper up to 800 grit, and one side of the specimen was coated with thin layer of nickel of less than 200nm. A solution containing 250g/l  $\text{NiSO}_4 \cdot 6\text{H}_2\text{O}$ , 45g/L  $\text{NiCl}_2 \cdot 6\text{H}_2\text{O}$  and 40g/L  $\text{H}_3\text{BO}_3$  was used as the coating solution, the coating current density was  $3\text{mA}/\text{cm}^2$ , and the coating time was 3min. It has been confirmed previously that the nickel-plated surface provide an advantages over a palladium-plated surface [9]. Before the test, the specimen was carefully cleaned with alcohol and acetone, then dried with cold wind, and then weighed.

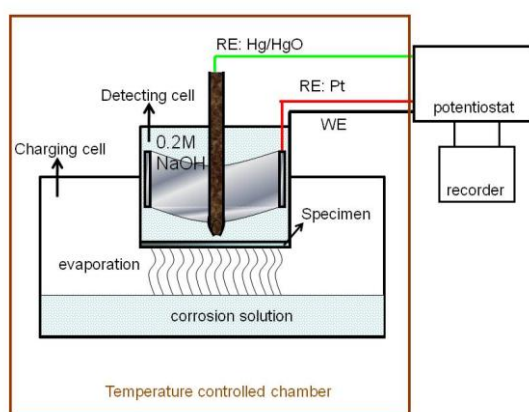


**Figure 1.** the schematic of experimental setup

### 2.2. Test procedures and permeation test

The test setup is shown in Fig.1. The two-component cell used for corrosion and permeation experiments is similar to Devnathan-Stachurski's electrolytic cell. Then the specimen was fixed to a

cell with the side with no nickel coating facing downward. The upper cell was filled with 0.2mol/l NaOH. Before hydrogen permeation test, the specimen was polarized potentiostatically at 150mV vs. HgO/Hg/0.2M NaOH for more than 24h until the remaining current density was less than 0.1 $\mu$ A/cm<sup>2</sup>. And then put the electrolytic cell onto a container which contained corrosion solution, the distance between the downwards specimen surface and the solution surface was about 20cm. At last, put the cell and container into a temperature controlled chamber. The temperature of the chamber was thermostatically controlled at 298K and the relative humidity is about 70%. Different concentration of SO<sub>2</sub> solutions were prepared by bubbling SO<sub>2</sub> gas in seawater that was deoxidized. After the hydrogen permeation experiment, the specimen was taken out, and the weight loss was measured after removing the rust layer.

SSRT test was carried out to measure the SCC sensitivity of steel.

### 2.3. Analysis of hydrogen permeation current

To estimate surface hydrogen content in the steel during the cyclic wet-dry process, we must know a hydrogen diffusion coefficient (D: cm<sup>2</sup>/s) of the steel at a given test temperature. The hydrogen diffusion coefficient was determined using a mathematical treatment which was developed for the permeation technique by McBreen [10] et al. And D can be obtained from the following equation

$$D = \frac{L^2}{6t_L} \quad (1)$$

Where L is the specimen thickness (cm) and the time of  $t_L$  corresponds to the point on the permeation curve at which  $\dot{i}_t = 0.63 \dot{i}^\infty$  which can be obtained from the experimental curves. And then hydrogen content ( $C_0$ ) can be calculated from equation (2).

$$C_0 = \frac{I^\infty L}{DF} \quad (2)$$

Where F (96500C/mol) is Faraday's constant.  $I^\infty$  (A/cm<sup>2</sup>) is the steady-state current density. L (cm) is the thickness of the specimen. The dimension in calculated  $C_0$  is mol/cm<sup>3</sup>.

The hydrogen permeated through the specimen can be calculated by integrating the area of hydrogen permeation current density.

### 2.4. D value for the specimen

The value of D is determined by D-S double cell. The specimen was used as public working electrode. The two cells were filled with 0.1M NaOH, and one was used as the cathodic charging cell, which was polarized at a constant current density -2mA/cm<sup>2</sup>. The other one was used as anodic cell and was kept at a constant potential of 0mV VS. Hg/HgO/0.1M NaOH. Hydrogen permeation current

was measured. This test was repeated three times and the average value was used in this paper. The  $D$  of the steel was  $3.12 \times 10^{-6} \text{ cm}^2/\text{s}$  at 293K.

### 3. RESULTS

#### 3.1. Hydrogen permeation experiment

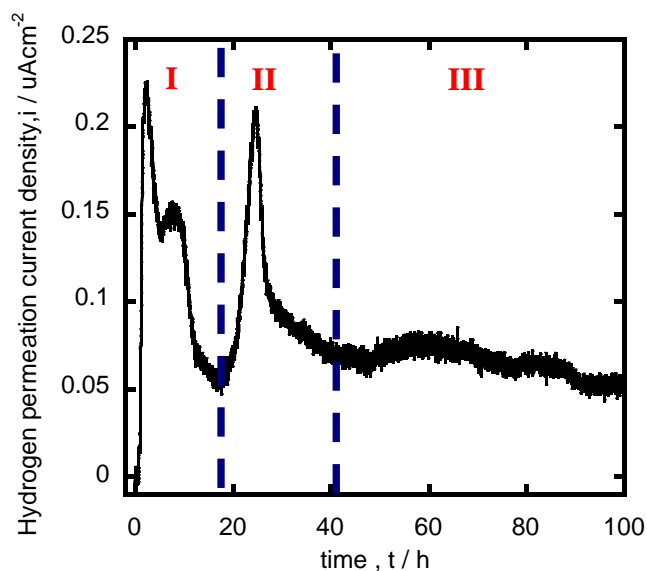


**Figure 2.** The hydrogen permeation current density of X56 steel in simulated marine atmospheric environment contain 0.01mol/L  $\text{SO}_2$

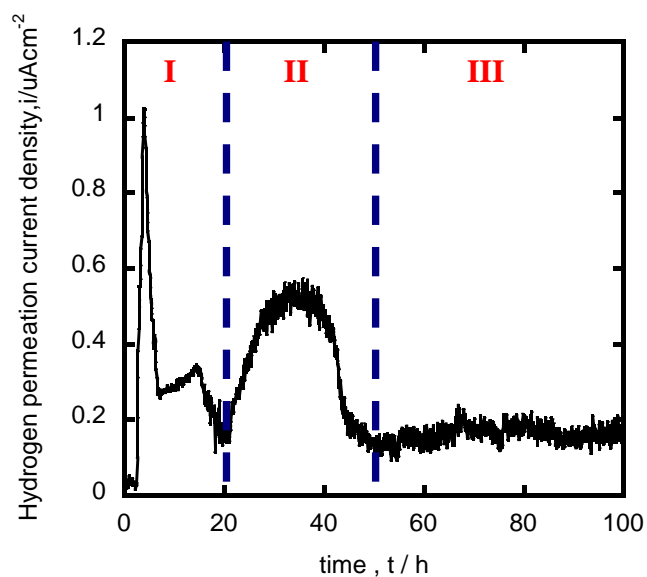


**Figure 3.** The hydrogen permeation current density of X56 steel in simulated marine atmospheric environment contain 0.03mol/L  $\text{SO}_2$

Fig.2 and Fig.3 show the hydrogen permeation current density of specimen in simulated atmospheric environment formed by 0.01mol and 0.03mol SO<sub>2</sub> solution. The plots can be divided into three stages as shown in the figures.

From these two figures, the hydrogen permeation current density increased sharply at the initial of the experiment, and then decreased quickly. After a short time stable value, the hydrogen permeation current density increased again and formed the second peak. After the second peak, the current density reached a relative stable value and last for a long time. And the hydrogen permeation current density increased while SO<sub>2</sub> concentration increases from 0.01mol to 0.03mol.

Fig.4 shows the surface hydrogen concentration calculated through equation 1 and 2.

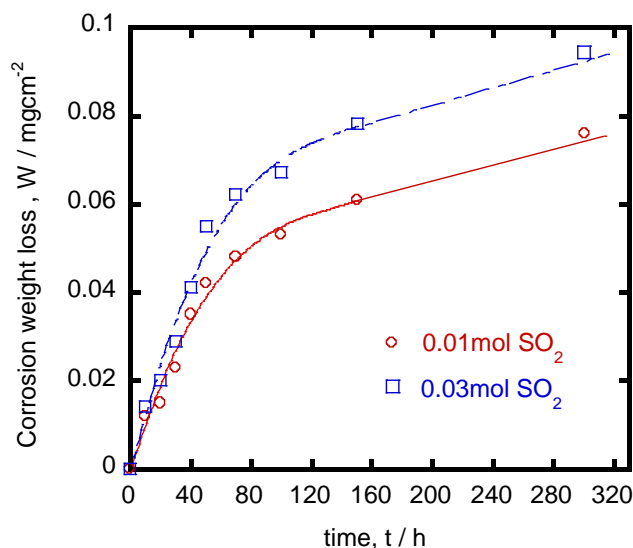


Figure 4. The corrosion weight loss of steel in different SO<sub>2</sub> concentration

3.2. Weight loss .

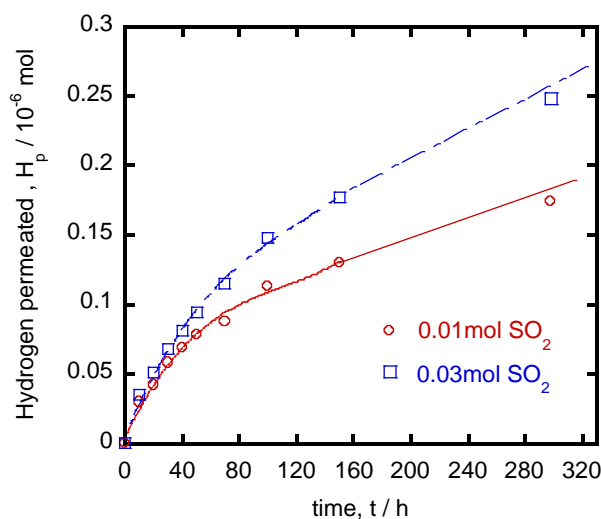
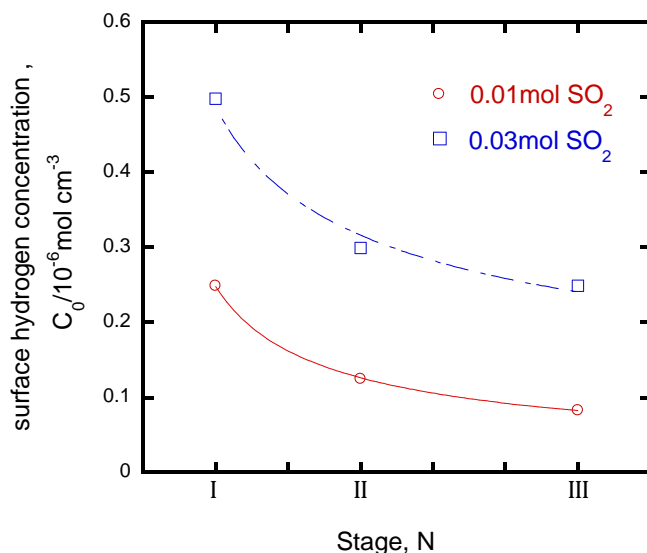
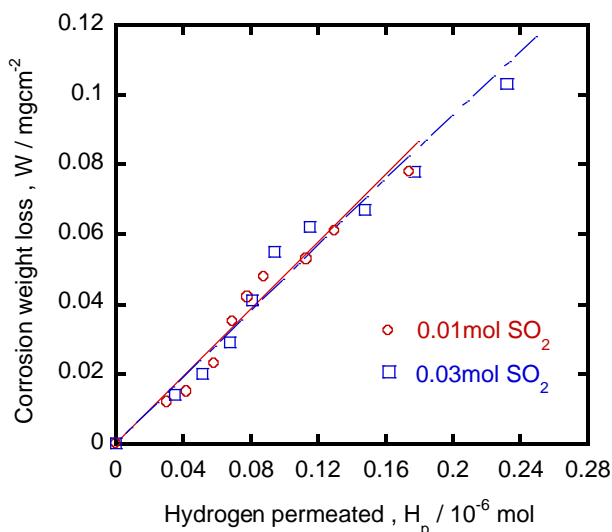


Figure 5. The amount of hydrogen permeated through the steel



**Figure 6.** the surface hydrogen concentration at different stage

Fig.5 shows the corrosion weight loss at different time. At the beginning of the experiment, corrosion weight loss increase quickly and then reached stable rate. This is mainly due to the protection effect of formed corrosion products. And corrosion rate of 0.03mol SO<sub>2</sub> formed atmospheric environment is bigger than 0.01mol SO<sub>2</sub> formed atmospheric environment. Fig.6 shows the amount of hydrogen permeated through the steel. It shows a similar trend with Fig.4. At first, the amount of hydrogen permeated through the steel increased quickly, and then the slope of increase decreased



**Figure 7.** The relation between amounts of hydrogen permeated and weight loss

Fig.7 shows the relationship between the weight loss and the quantities of the hydrogen permeated. A clear linear correlation exists between the quantities of hydrogen permeated through the X56 steel and the weight loss.

The cathodic reaction is the reduction of the oxygen dissolved into the water layer during the corrosion process. In this test, hydrogen evolution can be detected, this is evidence that the reduction of hydrogen ions occurs.

And the relationship in Fig.7 indicates the intrinsic relation of H<sup>+</sup> reduction with other possible corrosion processes including oxygen reduction. In the corrosion process, each reaction interacts and reaches quasi-equilibrium with others [11]. The hydrogen evolution is one among them, which the permeation current directly relates. The relationship between the weight loss and the quantities of the hydrogen permeated may help us to find a new and simple way to forecast corrosion degree and corrosion weight loss and monitor corrosion on-line.

3.3. SCC sensitivity of X56

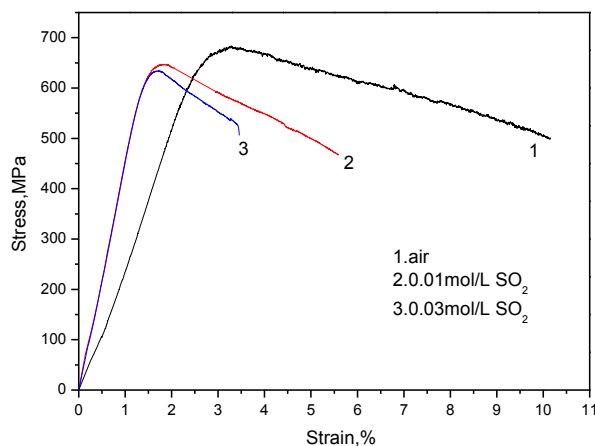


Figure 8. the stress-strain curves of X56 steel at various SO<sub>2</sub> concentration

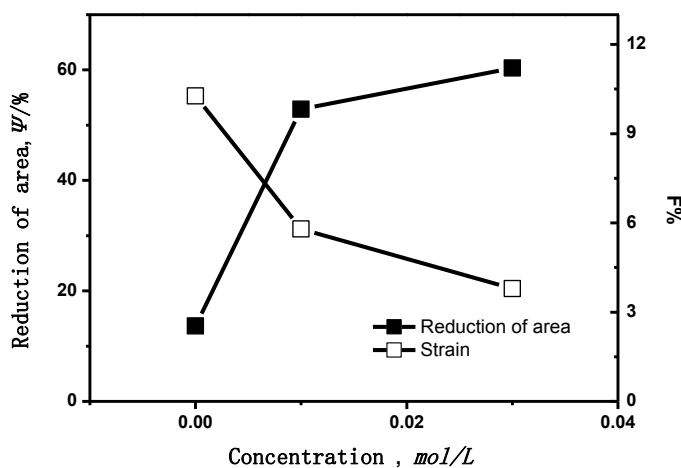


Figure 9. SCC sensitivity of X56 at various SO<sub>2</sub> concentration

SCC sensitivity of X56 was measured by SSRT in 0.01mol and 0.03mol SO<sub>2</sub> solution. The results are shown in Fig.8. The strain decrease sharply in 0.01mol SO<sub>2</sub> solution. The reduction of area

and strain are shown in Fig.9. The strain decrease with increasing of SO<sub>2</sub> concentration while reduction of area increase. This indicates the SCC sensitivity increase with increasing SO<sub>2</sub> concentration. And the difference of SCC sensitivity between 0.03mol and 0.01mol is little than between 0.01mol and air.

#### 4. DISCUSSIONS

Hydrogen permeation current plot can be divided into three stages as shown in the figure 2 and figure 3. After the experiment started, the main reactions occurred as (1), (2), (3) and (4) listed below. And these reactions are the main resource of hydrogen.



In these 4 reactions, much more hydrogen ion was generated suddenly, and induced the hydrogen permeation current increase sharply and after corrosion product film was formed, the hydrogen permeation current decrease.

At the same time, following reaction occurs



Fe<sup>2+</sup> can hydrolyze to FeOH<sup>+</sup> and Fe(OH)<sub>2</sub> which can be further oxidized to FeOOH by the following reactions[11]:



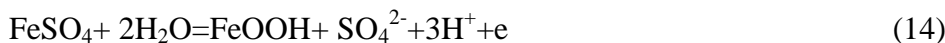
And SO<sub>3</sub><sup>2-</sup> can be further oxidized to SO<sub>4</sub><sup>2-</sup>.



And FeSO<sub>4</sub> formed by the following reactions:



From reactions 11 to 13, hydrogen cannot be produced through the formation of FeSO<sub>4</sub>. However, FeSO<sub>4</sub> can be further oxidized to FeOOH and generate H<sup>+</sup> ions.





From reactions 12 to 15,  $\text{SO}_4^{2-}$  was not consumed,  $\text{SO}_4^{2-}$  served as auto-catalyst, and more hydrogen ions were generated. So the second peak of hydrogen permeation current formed. In this case, if the autocatalysis always continues, the hydrogen permeation current density should show an increase trend always. However, the hydrogen permeation current kept a relative stable value after the second peak. This suggests that a part of  $\text{SO}_4^{2-}$  formed an insoluble compounds in the corrosion products and do not serve as auto-catalyst again. On the other hand, the film of corrosion products become thicker and thicker. According X-ray results of Nishimura [12], the weight percent of  $\text{Fe}_3\text{O}_4$  in the inner layer of the corrosion products is the largest (about 37%) after 300 hours corrosion. And the formation of  $\text{Fe}_3\text{O}_4$  would predominantly take place in the vicinity of substrate through 16, with production of  $\text{H}_2\text{O}$ , and make the corrosion products on the substrate would become dense and adherent as the inner layer. The corrosion products film can block the hydrogen ions moving to the metal surface, and increase the chance of combination of two hydrogen ions into hydrogen and then escape from the metal surface and corrosion rust layer[3].

From the above reactions, the main hydrogen source of each stage is of some different, supposing that: 1. Hydrogen permeation current at every stage in Fig.2 and Fig.3 is steady. 2. Ignoring the effect of corrosion products film on hydrogen permeation, the change of hydrogen permeation current only depend on the surface hydrogen concentration because corrosion products film wasn't formed at the beginning of the test. We can calculate the surface hydrogen concentration of each stage. Fig.4 shows the surface hydrogen concentration calculated through equation 1 and 2. The surface hydrogen concentration decrease with time, this suggests that the formation of corrosion products decrease the surface hydrogen concentration. There's no definite explanation for the effect of corrosion products on hydrogen permeation. There are several reasons such as the lower diffusivity of hydrogen in corrosion products, the increasing speed of combination reactions of hydrogen atoms and the lower coverage of hydrogen on the metal surface and so on. Anyway, corrosion products can block the hydrogen permeate into steel. And in this case, the surface hydrogen concentration decreased with time. And at the same time, the surface hydrogen concentration increase with the concentration of  $\text{SO}_2$ .

After the second peak, the current density reached a relative stable value and last for a long time. This suggested that the reaction of hydrolysis of  $\text{Fe}^{2+}$  and the block effect of corrosion products reached equilibrium. And at this stable step, the hydrolysis of  $\text{Fe}^{2+}$  is the main resources of hydrogen ions including reactions (5)-(18).



According the above, the mechanism of hydrogen permeation of steel in atmospheric environment containing  $\text{SO}_2$  can divided into 3 steps:

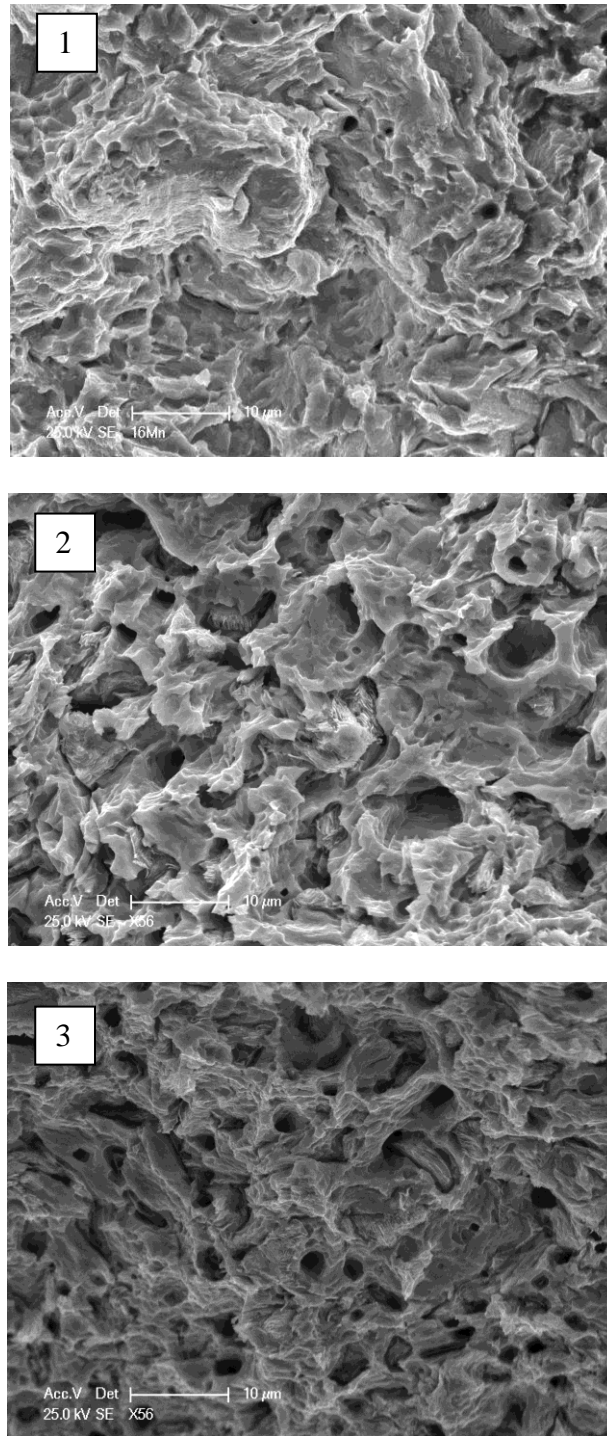


**Figure 10.** the SEM images of X56 steel in the simulated marine atmospheric environment (1)in air, (2) 0.01mol/LSO<sub>2</sub> and (3) 0.03mol/LSO<sub>2</sub>

1. The initial step. In this step, the hydrogen current increased quickly and the first peak was formed, the main resource of hydrogen ions is the hydrolysis of SO<sub>2</sub>.
2. The second step. The autocatalysis of SO<sub>4</sub><sup>2-</sup> provides the main resource of the hydrogen permeation current.

3. The steady step. In this step, the hydrolysis of  $\text{Fe}^{2+}$  and the blocking effect of the corrosion rust reach equilibrium. And hydrogen ions mainly come from the hydrolysis of  $\text{Fe}^{2+}$ . The hydrogen permeation current seems reached a stable value. This implies the hydrolyzation effect between all the reactions reached equilibrium, and the surface hydrogen concentration reached a stable value.

Comparing the results of hydrogen permeation test, the SCC of X56 steel was controlled by two factors, one is dissolve of the metal, the other one is hydrogen induced fracture. Fig.10 shows the SEM images of fracture surface which also shows some characteristic of hydrogen induced fracture.

## 5. CONCLUSIONS

1) Hydrogen permeation current can be divided into 3 parts in atmospheric environment containing  $\text{SO}_2$ . Initial peak, second peak and steady step. And hydrolysis of  $\text{SO}_2$ , autocatalysis of  $\text{SO}_4^{2-}$  and the hydrolysis of  $\text{Fe}^{2+}$  are the resources for each step respectively.

2) The surface hydrogen ions concentration decrease with time. And this indicates that the surface hydrogen concentration decrease with the formation of corrosion rust. The formation of  $\text{Fe}_3\text{O}_4$  would predominantly take place in the vicinity of substrate, and the corrosion products on the substrate would become dense and adherent as the inner layer.

3) SEM and Slow strain rate test (SSRT) shows that SCC sensitivity of X56 increase with the concentration of  $\text{SO}_2$  due to the passivation film dissolves and hydrogen permeation rate increasing.

## ACKNOWLEDGEMENTS

This work was financially supported by the Natural Science Foundation of China (NO.51001055) and The Priority Academic Program Development of Jiangsu Higher Education Institutions.

## References

1. H. E. Townsend, *Corro.*, 28(1972), 39.
2. A. Ikeda, T. Kaneko and F. Terasaki, *Corro.*, 80(1980), 8.
3. C. B. Zheng, Y.L. Huang, C.Y. Huo, Q. Yu, *Mater. Corro.*, 5(2007), 716.
4. N.B. Bhosle, , A.B. Wagh, *Corro. Sci.*, 33(1992),647.
5. V. K. van Gelder, J.G. Erlings, J.W.M. Damen, A. Visser, *Corro. Sci.*, 27(1987), 1271.
6. M. Barteri, F. Mancina, A. Tamba, and G. Montagna, *Corro. Sci.*, 27(1987), 1239.
7. T. Kushida, *ISIJ International*, 43(2003), 470.
8. C. B. Zheng, Y. L. Huang, Q. Yu, C.Y. Huo, *Corro. Eng. Sci. Techn.*, 44(2009), 96.
9. W.C. Luu, H. S. Kuo and J. K. Wu, *Corro. Sci.*, 39(1997), 1051.
10. J. McBreen, L. Nonis, and W. Beck, *J. Electrochem. Soc.*, 113(1966), 1218.
11. Y.L. Huang, Y.Y. Zhu, *Corro. Sci.*, 47(2005),1545.
12. R. Nishimura, D. Shiraishi, Y. Maeda, *Corro. Sci.*, 46(2004), 225.